CLM-P208

United Kingdom Atomic Energy Authority
RESEARCH GROUP

Preprint

LASER INTERFEROMETRY IN THE PRESENCE OF TRANSVERSE PLASMA DENSITY GRADIENTS

S. S. MEDLEY

Culham Laboratory
Abingdon Berkshire

1969

UNCLASSIFIED
(Approved for Publication)

CLM - P 208

LASER INTERFEROMETRY IN THE PRESENCE OF TRANSVERSE PLASMA DENSITY GRADIENTS

by

S.S. MEDLEY*

(Submitted for publication in J. Applied Physics)

*On leave of absence from:
Department of Physics,
University of British Columbia,
Vancouver, British Columbia

U.K.A.E.A. Research Group,
Culham Laboratory,
Abingdon,
Berks,
July, 1969

ABSTRACT

A novel laser interferometric technique involving the use of an unstable external resonator is presented. The unstable resonator greatly facilitates electron density measurements in the presence of plasma density gradients transverse to the direction of beam propagation. The technique is used to obtain time-resolved radial electron density distributions in the implosion stage of a linear z-pinch discharge in argon at filling pressures of 100 and 1000 Torr.

CONTENTS

ERRATUM

For pressure unit Torr read milli-torr throughout

I. INTRODUCTION

Since the introduction of the laser interferometer in 1963 by Ashby and Jephcott[1,2], several modifications have been made which extend the usefulness of the device[3-9]. Of particular importance in the investigation of fast, pulsed plasmas is the extension of the interferometer frequency response[10,11]. All of the previous interferometers, however, have a common shortcoming: large gradients of electron density transverse to the direction of beam propagation preclude their application. Such gradients act, to a first approximation, as a prism to bend the laser beam in the direction of decreasing electron density. This causes misalignment of the interferometer and, in many cases, completely prevents measurement due to deflection of the beam out of the transversely finite mirror structure.

This paper describes a technique which facilitates application of the laser interferometer to electron density measurements in the presence of plasma density gradients. Analysis of beam behaviour in a resonator containing a plasma with a simple transverse gradient of electron density yields, in the approximation of ray optics, two conditions to maintain interferometer alignment. First, the centre of curvature of the spherical external mirror must coincide with the axial midpoint of the plasma. This necessitates operating the external resonator in an unstable regime. Second, provision must be made to reduce the path length of the laser beam through the plasma. The former condition is

readily satisfied in general, but the latter requires the nature of the plasma under investigation to be considered. A method suitable for adjusting the path length for a beam propagating parallel to the axis of a z-pinch discharge is presented.

The technique is used to obtain time-resolved radial electron density distributions for the implosion stage of a linear z-pinch discharge. The discharge vessel is 62 cm in length and of 15 cm bore. A capacitor bank energy of 3.6 kJ and a charging voltage of 12 kV are used. At argon filling pressure of 100 and 1000 Torr, this gave times to pinch of 5 and 13 μsec, respectively, with peak electron densities of the order of 10^{17} cm^{-3}.

II. MAINTAINING INTERFEROMETER ALIGNMENT IN THE PRESENCE OF A TRANSVERSE DENSITY GRADIENT

The problem to be considered is the behaviour of a laser beam in a resonator containing a medium in which the refractive index, n, has a constant gradient, $\partial n/\partial r$, transverse to the resonator axis. Under such conditions, a beam of light travelling parallel to the resonator axis will be bent through an angle[12]

$$\varepsilon = \int_0^L \frac{1}{n} \frac{\partial n}{\partial r} \, dz \qquad \ldots (1)$$

from its original direction. Here the integral is taken in the z (axial) direction over the beam path length, L.

Fig.1 illustrates the problem. The coordinate system (r,z) is defined by the plane mirror and the resonator axis. A slab of plasma of axial length, L, is situated in the resonator and has a 'radial' gradient of refractive index as indicated.

Consider a beam which is launched from the plane mirror at an angle θ_o and with a displacement r_o relative to the resonator axis. The subsequent history of the beam, using the approximation of geometrical optics for paraxial rays and neglecting refraction at the plasma boundaries, is as follows. On passing through the plasma, the beam undergoes an angular deflection ε (away from the axis for positive $\partial n/\partial r$) and consequently a radial displacement from the axis. The beam is incident on the spherical mirror at an angle

$$\theta' = \theta_o + \varepsilon \qquad \ldots (2)$$

with a displacement

$$r' = r_o + \theta_o d + \varepsilon\left(\frac{L}{2} + d_1\right) \qquad \ldots (3)$$

relative to the axis. Here d is the axial length of the resonator and d_1 is the axial distance from the spherical mirror to the nearer boundary of the plasma slab. The reflected beam is again deviated and displaced, returning to the plane mirror at an angle

$$\theta_1 = \frac{2r_o}{R} + \theta_o\left(\frac{2d}{R} - 1\right) + 2\varepsilon\left(\frac{\frac{L}{2} + d_1}{R} - 1\right) \qquad \ldots (4)$$

with a displacement

$$r_1 = r_o\left(1 - \frac{2d}{R}\right) + 2\theta_o d\left(1 - \frac{d}{R}\right) + 2\varepsilon d\left(1 - \frac{\frac{L}{2} + d_1}{R}\right) \qquad \ldots (5)$$

where R is the radius of curvature of the spherical mirror. In these equations, the curvature of the beam path in the plasma is taken into account to a first order in the gradient of the refractive index. Note that for $R \to \infty$ these equations reduce to the obvious result for a resonator with plane parallel mirrors.

Alignment of the laser interferometer requires that, after a discrete number[3] of traversals through the resonator, the beam retrace itself to its initial launching point. The interferometer as used here is initially aligned so that $r_o = 0$, $\theta_o = 0$ in the absence of plasma. In this case, it can be seen from Eqs. (4) and (5) that after a double pass with the plasma present, the beam returns to the plane mirror along its initial trajectory provided

$$R = \frac{L}{2} + d_1 \ . \qquad \ldots (6)$$

This result has a simple physical interpretation. When the

above equation is satisfied, the radius of curvature of the spherical mirror coincides with the axial midpoint of the plasma slab. As a result, the deflected beam is, to a good approximation, normally incident at the spherical mirror and consequently returns on the same path. However, this argument presupposes the beam does not miss the spherical mirror on the first pass. Therefore, the following restriction must be imposed on the maximum permissible angular deflection:

$$\varepsilon_{max} < \frac{a}{\sqrt{a^2 + R^2}} \qquad \ldots (7)$$

where a is the radius of the aperture which limits the transverse motion of the beam in the interferometer (here taken to be the external mirror). For small angular deflections, Eq.(1) can be approximated by

$$\varepsilon = \frac{L}{n} \frac{\partial n}{\partial r} \qquad \ldots (8)$$

where $\partial n/\partial r$ is understood to be the average value along the beam path. Since for a plasma $n \cong 1$, Eq.(7) can be expressed in the form

$$L_{max} < \frac{a}{\sqrt{a^2 + R^2}} \left(\frac{\partial n}{\partial r}\right)^{-1}. \qquad \ldots (9)$$

To satisfy this inequality for a fixed but unknown radial gradient of refractive index, the path length, L, of the

beam through the plasma must be adjustable. Thus, a further condition imposed by alignment requirements is that the length of the beam path through the plasma be variable. The manner in which this was accomplished in the case of a z-pinch discharge is discussed in Sec.III.

If Eqs. (6) and (9) (hereafter called the alignment conditions) are satisfied, the laser beam will remain aligned in the external resonator in spite of a radial gradient of refractive index of the plasma medium. Some experimental implications of the alignment conditions require further discussion.

Optical resonators are classified as stable or unstable depending, respectively, on whether the beam is refocused or transversely dispersed upon being periodically redirected by the resonator mirrors. A resonator is stable when the inequality[13]

$$0 < \left[1 - \frac{d}{b_1}\right]\left[1 - \frac{d}{b_2}\right] < 1 \qquad \ldots (10)$$

is satisfied: otherwise it is unstable. Here b_i is the radius of curvature of the i-th resonator mirror and d is the axial length of the resonator. Since for the present resonator, $b_1 = R$ and $b_2 = \infty$, the stability criterion is simply

$$0 < 1 - \frac{d}{R} < 1 \, . \qquad \ldots (11)$$

It is clear that in order to satisfy the alignment condition specified by Eq. (6), the resonator must necessarily be operated in the unstable regime.

It should be remarked that the stability concept has the following interpretation in the context of the distribution of fields in a resonator. The fields of modes in unstable resonators are less concentrated near the axis than those of stable resonators. Consequently, the diffraction losses at the mirrors are much higher for unstable resonators[14] than they are for stable resonators. However, a lossy resonator is advantageous[15] for interferometry at high frequencies ($f > 1$ MHz) such as are commonly encountered in pulsed plasma work and therefore presents no difficulty in the intended application.

Shortening the path length, L, of the beam through the plasma in order to limit the maximum angular deflection has the concomitant disadvantage of degrading the interferometer sensitivity. The number, N, of interferometer fringes produced by a change in electron density $\bar{n}_e$, averaged over the beam path, is given by[16]

$$N = \frac{e^2}{m\varepsilon_o\omega^2} \cdot \frac{L}{\lambda} \cdot \left| \bar{n}_e(t_1) - \bar{n}_e(t_o) \right| \cdot \qquad \ldots (12)$$

This equation is valid only for monotonically increasing or decreasing electron density throughout the time interval $t_1 - t_o$. At optical frequencies, the index of

refraction of an electron gas with density n_e is given by

$$n = \left[1 - \frac{\omega_p^2}{\omega^2} \right]^{\frac{1}{2}} \simeq 1 - \tfrac{1}{2} \frac{e^2}{m\varepsilon_o \omega^2} \cdot n_e . \quad \ldots (13)$$

Using the above expressions, it is easily shown that the path length restriction of Eq.(9) implies the following limitation on the total number of fringes obtainable:

$$N_{max} < \frac{2}{\lambda} \cdot \frac{a}{\sqrt{a^2 + R^2}} \cdot \frac{|\bar{n}_e(t_i) - \bar{n}_e(t_o)|}{\partial n_e / \partial r} \cdot \quad \ldots (14)$$

In practice, at least 10 fringes can usually be obtained which is adequate for electron density measurements to within 5% with the existing uncertainty in N of 1/2 of a fringe.

III. EXPERIMENTAL APPARATUS

The Interferometer

An interferometer of the Ashby-Jephcott-Gerardo type, shown schematically in Fig.2, is used.[11] The laser (Spectra Physics Model 116, CW He-Ne) and the spherical external mirror (radius of curvature, 2 m; aperture radius, 1.9 cm; reflectivity 60% at $\lambda = 0.63\mu$) are mounted at opposite ends of an aluminium channel which is 5 m long, 20 cm wide, 8 cm deep and of 1 cm thickness. The external mirror is held in the vertical plane by a 3-point support provided with spring-loaded differential screws for mirror alignment. A 2 cm diameter hole at the back

of the mirror mount allows the laser radiation transmitted through the resonator to be received by a 150 CVP photomultiplier having a measured risetime of 8 nsec. Optical pick-up due to plasma radiation is reduced by means of iris diaphragms and an interference filter which is centered at the laser wavelength ($\lambda = 0.63\mu$).

The interferometer is supported at either end by lateral travelling screw arrangements fitted to vertically adjustable tables. Thus the optical assembly could be moved, as a whole, independently of the discharge vessel which is situated between the laser and the external mirror. This enabled easy alignment of the laser beam parallel to the discharge axis at any desired radius without disturbing the interferometer alignment.

The frequency response of the combined laser interferometer and ancillary detection equipment was measured *in situ* by rotating a fused-quartz plate in the path of the laser beam in the external resonator. The plate, of dimensions 1.25 cm x 2.50 cm x 3.00 cm with the large faces polished flat to $\lambda/20$ and parallel to one second, had a maximum speed of 25,000 rpm. The fringe amplitude (normalized at 1 MHz) was observed to fall to 10% depth of modulation at 40 MHz.

The rotating plate also served to calibrate the sensitivity of the interferometer. Using Snell's Law and assuming that one fringe corresponds to $\lambda/2$ change

in resonator optical length, the fringing rate was calculated as a function of plate rotation speed. The good agreement between observed and calculated fringing rate verified the assumed sensitivity. It may therefore be concluded that only the lowest order (TEM_{ooq}) modes are, in fact, resonant since if higher modes were present this correlation would not occur.[17]

The Discharge

The linear z-pinch discharge used in this investigation is of conventional design[18,19] with the exception of the discharge vessel which is described in detail.

A scale diagram of the discharge vessel is given in Fig.3. The electrodes are 0.3 mm thick brass discs with a diametrical slot 1 cm wide and extending to within 1.5mm of the disc edge. The slots, which are aligned horizontally parallel in the discharge vessel, allow the laser beam to pass through the discharge. Also, the slots accommodate two glass tubes which are inserted into the plasma; one through each electrode. The tubes are open-ended lengths of ordinary silica glass tubing (8 mm o.d., 6 mm i.d.) with the ends polished square. They are separately mounted in rack-and-pinion holders which, in turn, are mounted externally to the plasma behind the discharge electrodes. The holders permit adjustment of the radial position and axial separation, L, of the tubes.

Two 6 mm diameter ports, one approximately 7 cm

from each electrode and both on the same side of the discharge vessel, permit insertion of two graduated rods across the diameter of the vessel and parallel to the electrode slots. The rods, graduated in 0.05 mm divisions, are used to align the laser beam parallel to the axis of the discharge vessel.

The axes of the tubes are aligned coincident with that of the external resonator which, in turn, is parallel to (but, in general, not coincident with) the discharge axis. Thus the laser beam propagates axially within the tube bore and is shielded from the plasma except over a path of variable length, L. This arrangement served to satisfy the inequality (9).

IV. EXPERIMENTAL RESULTS

The technique described above was used to obtain time-resolved radial distributions of electron number density for the implosion stage of the z-pinch discharge at argon filling pressures of 100 and 1000 Torr. The quantity measured directly is the electron density averaged over the axial path length, L, of the discharge as a function of time after initiation of the discharge current. Typical oscillograms are shown in Fig.4. The current waveform was usually displayed at a sweep rate of 2 μsec/cm while the fringe pattern was displayed at 0.2 μsec/cm over an interval of time corresponding to the intensified segment on the current trace. Measurements were made at 2 mm radial intervals over most of the discharge vessel

radius (75 mm).

The manner in which the fringe patterns were interpreted is illustrated in the self-explanatory diagram of Fig.5. Recall that the relation between electron density and the number of fringes (Eq.12) is valid only for electron density which is increasing or decreasing monotonically with time. Such is not the case in the present investigation. However, during the implosion stage of the z-pinch discharge, the electron density at any specified radius is expected to increase monotonically from zero to a maximum value, called the 'turnover', and thereafter monotonically decrease. In this case, Eq.(12) can be applied simply by counting the fringes in the manner prescribed. Interpretation of the fringe pattern is therefore relatively straightforward, the only difficulty being perhaps in identification of the turnover.

In general, the turnover is characterized by one of two features on the fringe pattern, depending on the optical length of the resonator at the moment turnover occurs. If the optical length is such that the transmission of laser radiation through the resonator is near-maximum or near-minimum, the turnover will occur at an extrema of the fringe amplitude. In this case, a flat segment appears at the 'centre' of the fringe pattern as illustrated in Fig.4a. On the other hand, if turnover occurs when the transmission is somewhere between the extrema, a sudden reversal in the direction of intensity variation

results as is shown in the trace of Fig.4b.

For the above interpretation of the fringe pattern to be consistent, the number of fringes on either side of the turnover should be equal to within 1/2 of a fringe, the accuracy of the fringe count. This in fact was the case for all measurements except those for near-axial radii where the decreasing portion of the fringe count defied interpretation due to the complicated behaviour of the plasma subsequent to the initial pinch.

Fig.6 shows the variation of electron density at selected radii as a function of time after current initiation (temporal profiles) for a discharge in argon at 100 Torr.

Fig.7 is obtained by plotting against each radial position of measurement the time at which peak electron density occurs (for the associated temporal profile). The peak density points have a scatter of ± 0.2 μsec about the smooth 'density implosion' curve drawn, the scatter being attributed to experimental inaccuracy in determining the start of the fringe pattern relative to the time of current initiation (Fig.5). However, a relative shift of ± 0.2 μsec in the time scale of individual temporal profiles produces a large scatter (typically 20%) in the electron density values for the subsequently determined radial profiles. Explanation of the manner in which this scatter arises is given by way of the following example.

Typically, the temporal profiles exhibit a rate of change of electron density of the order of 10^{17} $cm^{-3}\mu sec^{-1}$. Consequently, in reading the electron density from these curves at a specified time, a jitter of 0.2 μsec results in a fluctuation of 0.2×10^{17} cm^{-3} in the value of electron density. Since the electron densities measured are the order of 10^{17} cm^{-3}, the scatter in values amounts to about 20%. To circumvent this difficulty, before extracting the radial profiles each temporal profile was shifted in time by an amount necessary to make the peak coincide with the smooth density implosion curve. In most cases, the time shifts required were the order of 0.1 μsec.

Becuase the implosion stage of the discharge is reproducible, it is possible to combine the temporal profiles at different radii to obtain the radial distribution of electron density at a specified time after current initiation. The radial profiles are obtained simply by reading the electron densities corresponding to a selected time after current initiation from each of the temporal profiles. Radial profiles for a discharge in argon at 100 Torr and having a time-to-pinch of 5 μsec are given in Fig.8. Results similar to those presented above but for a filling pressure of 1000 Torr are shown in Fig.9.

It is worth while to note an interesting feature of the radial profiles at 100 Torr pressure. As the pinch develops, but before the imploding shell has reached the axis, the electron density profiles exhibit two peaks.

One peak coincides with the imploding shell while the other is apparently centered on the discharge axis. Once the column is fully pinched, only one peak is observed. Since detailed measurements in the immediate axial region could not be obtained with the existing equipment, it is difficult to advance an explanation of the inner peak, which is at present being further investigated.

V. EXPERIMENTAL DETAILS

In the z-pinch discharge, both the slots in the electrodes and the glass tubes inserted through them are potential sources of perturbation on the formation of the plasma column. To investigate their effect, a high speed framing camera was used to photograph the discharge.

The effect of the slotted electrodes on the cylindrical symmetry of the plasma column was investigated by taking side-on photographs of the discharge viewing simultaneously in directions parallel and perpendicular to the slots. Measurement of the outer luminous diameter of the plasma showed an ellipticity (major axis parallel to the slots) which never exceeded 3% and diminished as the column imploded.

The sequence of photographs in Fig.10 shows the central region of the discharge for a filling pressure of 100 Torr and a 2.5 cm gap between the tube ends. Successive exposures are staggered with time increasing in the direction of the arrow. In film sequence (a), the tubes are

2.5 cm from the discharge axis and become visible when the plasma shell arrives at their radial position. The pinch subsequently forms in the usual manner along the entire length of the discharge axis. However, when the tubes are aligned to within their radius from the discharge axis as in film sequence (b), the pinch forms in the usual manner only along the axial segment between the ends of the tubes. Therefore, on the basis on photographic evidence, it can be stated that: (1) the slotted electrodes do not significantly perturb the cylindrical symmetry of the plasma column so that measurements can be made at any azimuthal position without loss of generality, and (2) the presence of the glass tubes inserted into the discharge produces no apparent disturbance of the plasma in the region between the tube ends where measurement is performed.

A further check on the effect of the glass tubes on the electron density measurement relies on the fact that the ratio N/L (Eq.12), and hence the measured electron density, should be independent of the length, L, of plasma used. This check is valid provided the axial variation of electron density is below the sensitivity limit of the measurement for the particular path length used. For the measurements reported here, the ratio N/L is independent of L to within the experimental accuracy of 10%. However, for the case of 100 Torr filling pressure the scaling check failed for radii less than 4 mm, as demonstrated in Table I.

TABLE I. SCALING CHECK (100 TORR ARGON)

Discharge radius r(cm)	Path Length L(cm)	Maximum Fringe Number, N	N/L
5.0	60	9	.15
	40	6	.15
4.0	42	10	.24
	31	7	.23
3.0	31	12	.39
	25	10	.40
2.0	15	10	.67
	12.5	8	.64
	10	7	.70
1.0	6.5	11	1.5
	5.0	9	1.8
	3.8	6	1.6
0.0	3.0	4	1.3
	2.5	5	2.0
	1.0	4	4.0

Similar failure occurred for 1000 Torr at radii less than 14 mm. Data for which the scaling check failed were regarded as unreliable and consequently rejected.

Several effects may introduce error into the measured value of electron density- for example, uncertainty in the fringe count, reproducibility of the z-pinch discharge and contributions to changes in the index of refraction from sources other than the electron number density.

Evidence based on the scaling check discussed above indicates that, except for near-axial measurements, the

the glass tubes do not significantly perturb the plasma in the region between the ends. The length of the plasma through which the laser beam travelled was therefore taken to be the distance separating the tube ends. The uncertainty in L, which was easily measured to within 1 mm using a vernier calliper, never exceeded 3% and was typically less than 1%. Consequently, the error introduced into the electron density measurement due to uncertainty in the path length was regarded as negligible.

An error in the total fringe count of 1/2 of a fringe is always present due to the fact that structural vibrations in the optical system cause a continual variation in the optical length of the resonator. The period of the 'structural' fringes is long (>50 μsec) compared with the time interval of the measurement (<5 μsec). Hence the structural vibrations do not contribute to the fringe count directly. However, due to such vibrations, the start of the fringe count is known only to within an accuracy of 1/2 of a fringe. In general, the total fringe count was greater than 10 and therefore accurate to within 5%. Consequently, no effort was made to suppress the structural fringes and, in fact, they were utilized to optimize alignment of the interferometer.

The reproducibility of the discharge current was examined by superimposing several current waveforms on the same oscillogram, two for the glass tubes inserted on-axis and two for the tubes removed. The waveforms coin-

cided to within the width of the oscilloscope trace. Therefore it can be stated that the discharge current is very reproducible and furthermore, the presence of the glass tubes did not significantly affect the inductance associated with the pinched plasma column.

A further check on the plasma reproducibility was provided by obtaining several fringe patterns for the same experimental conditions. Direct comparison of the patterns by superposition was not possible due to the randomness of the fringe starting point discussed above. Instead, the corresponding temporal profiles were compared. For profiles obtained at radii greater than 2 cm, the peak electron densities agreed to within 10% and coincided in time to within 0.2 μsec. At smaller radii, the peaks still coincided in time to within 0.2 μsec, but the density values agreed only to within 20%.

In a plasma medium the index of refraction is determined by all constituents of the plasma: i.e. atoms, ions and electrons. In practice, however, the contribution to the refractivity by the free electrons dominates the contribution by all other constituents except perhaps the ground state atoms. If the laser frequency nearly coincides with a transition frequency of the ground state atoms, they may give a large contribution to the refractivity due to the phenomenon of anomalous dispersion. However, in the case of argon discharges the resonance wavelengths occur in the far ultraviolet so this effect will not be

encountered here. The effect of a change in neutral gas density (for example, due to a non-ionizing shock front preceding the plasma shell) merits further consideration.

The refractivity of argon as a function of density and wavelength is given by[20]

$$n_a - 1 = \left[1.03 \times 10^{-23} + \frac{0.58 \times 10^{-33}}{\lambda^2} \right] Na \quad \ldots (15)$$

where λ is in cm and the neutral gas density N_a is in cm^{-3}. Recalling that a change of $\lambda/2$ in the optical length of the resonator produces one fringe, the number of fringes resulting from a change Δn_a in the refractive index of the neutral gas is therefore

$$N = \frac{\Delta n_a \cdot L}{\lambda/2} \quad . \qquad \ldots (16)$$

Consider the case of a strong, non-ionizing shock propagating in argon at 100 Torr and at room temperature. The limiting density ratio across the shock front is 4 and the corresponding change in refractive index is $\Delta n_a = 10^{-7}$, using the ideal gas law to give $N_a = 3.8 \times 10^{15}$ cm^{-3} for the stated conditions. For measurement using the full length of the discharge (L = 62 cm), this change in refractive index produces 1/5 of a fringe. Since the sensitivity of the interferometer is the order of 1/2 of a fringe, it can be concluded that the refractive index contribution to fringes from neutral argon ahead of the

imploding shell is negligible.

If the shell is a region of strong ionisation, then it must also be a region of very low neutral argon density and the possibility of fringes due to the decrease in this density must be considered. However, even for full ionisation the change of neutral argon refractive index is less than for the above case of the shock wave. Hence this effect is of no consequence.

In view of the preceding discussion, it can be stated that the principal sources of error were reproducibility of the plasma and uncertainty in the fringe count due to structural vibrations of the interferometer system. In general, measurements obtained at radii greater than 2 cm were accurate to within 10% while those obtained at smaller radii were accurate to within 20%.

VI. CONCLUSIONS

Use of an unstable external resonator has enabled laser interferometric measurement of electron density ($\sim 10^{17}$ cm^{-3}) in the presence of transverse density gradients of at least $\frac{\partial n_e}{\partial r} = 2 \times 10^{17}$ cm^{-4}. With a conventional stable resonator, on the other hand, measurement was feasible only when the density gradient was smaller by an order of magnitude or more.

The stated gradient represents the limit for the present apparatus rather than the technique. Larger gradients may be dealt with by use of a larger aperture,

smaller radius of curvature external mirror in order to relax the limitation on the maximum permissible angular deflection (Eq.7).

A practical limit to the maximum tolerable gradient is imposed by spatial resolution considerations. If over the length of the plasma the displacement of the beam trajectory is, say, greater than the beam diameter, then spatial resolution may be regarded as seriously degraded. For the results reported, the beam displacement in the plasma never exceeded 0.5 mm with a beam diameter of ~ 2 mm, hence the spatial resolution was not significantly impaired.

ACKNOWLEDGMENTS

This work was supported financially by the Atomic Energy Control Board of Canada and the National Research Council of Canada. The author wishes to acknowledge the technical assistance of J. Dooyeweerd, A. Fraser, T. Knopp and J. Lees in the construction of the apparatus. Particular thanks are due to Dr. F.L. Curzon, Dr. A. Folkierski and Dr. J.H. Williamson for many useful discussions and suggestions.

REFERENCES

1. D.E.T.F. Ashby and D.F. Jephcott, Appl. Phys. Letters 3, 13 (1963).

2. D.E.T.F. Ashby, D.F. Jephcott, A. Malein and F.A. Raynor, J. Appl. Phys. 36, 29 (1965).

3. J.B. Gerardo and J.T. Verdeyen, Proc. I.E.E.E. 52, 690 (1964).

4. D.A. Baker, J.E. Hammel and F.C. Jahoda, Rev. Sci. Instr. 36, 395 (1965).

5. A. Gibson and G.W. Reid, Appl. Phys. Letters 5, 195 (1964).

6. W.A. Kricker and W.I.B. Smith, Phys. Letters 14, 102 (1965).

7. H. Malamud, Rev. Sci. Instr. 36, 1507 (1965).

8. E.B. Hooper and G. Bekefi, J. Appl. Phys. 37, 4083 (1966).

9. R. Turner and T.D. Poehler, J. Appl. Phys. 39, 5726 (1968).

10. C.B. Wheeler and A.E. Dangor, AGARD Conference Proceedings No.8, Vol.2, 517 (1965).

11. J.B. Gerardo, J.T. Verdeyen and M.A. Gusinow, J. Appl. Phys. 36, 2146 (1965).

12. U. Ascoli-Bartoli, in 'Plasma Physics' (Lectures at Trieste, October 1964), (International Atomic Energy Agency, Vienna, STI/PUB/89, 1965). p.287.

13. H. Kogelnik and T. Li, Appl.Opt. 5, 1550 (1966).

14. W.K. Kahn, Appl.Opt. 5, 407 (1966).

15. J.H. Williamson and S.S. Medley, Can. J. Phys. 47, 515 (1969).

16. J.B. Gerardo, J.T. Verdeyen and M.A. Gusinow, 'Theory of the Laser Interferometer and its Use in Plasma Diagnostics', Scientific Report No.1, Grant No. DA-ARO-D-31-124-G582, University of Illinois Urbana, Illinois (1964).

17. J.T. Verdeyen, J.B. Gerardo and E.P. Bialecke, Proc. I.E.E.E. 51, 1775 (1963).

18. S.S. Medley, F.L. Curzon and C.C. Daughney, Rev. Sci. Instr. 36, 713 (1965).

19. S.S. Medley, F.L. Curzon and C.C. Daughney, Can. J. Phys. 43, 1882 (1965).

20. U. Ascoli-Bartoli, A. De Angelis and S. Martellucci, Nuovo Cimento 18, 1116, (1960).

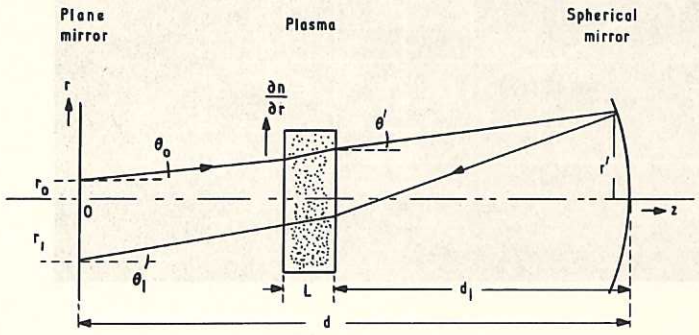

Fig. 1 (CLM-P 208)

Schematic diagram of resonator containing plasma having a transverse gradient of electron density

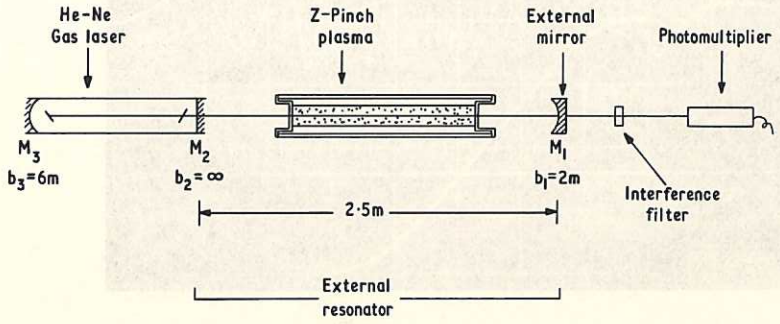

Fig. 2 (CLM-P 208)

Schematic arrangement of the laser interferometer

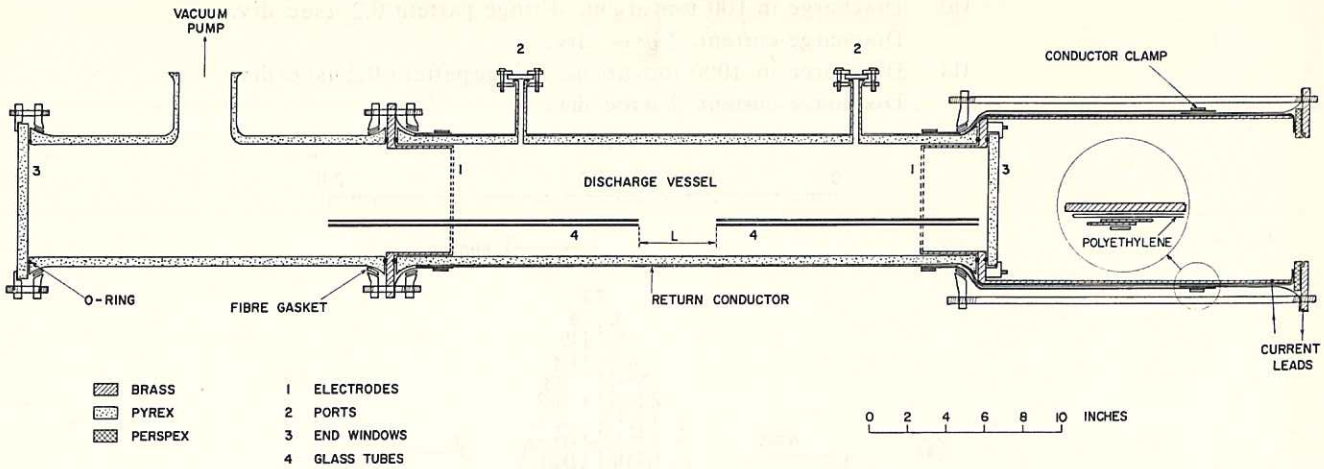

Fig. 3 Details of the z-pinch discharge vessel (CLM-P 208)

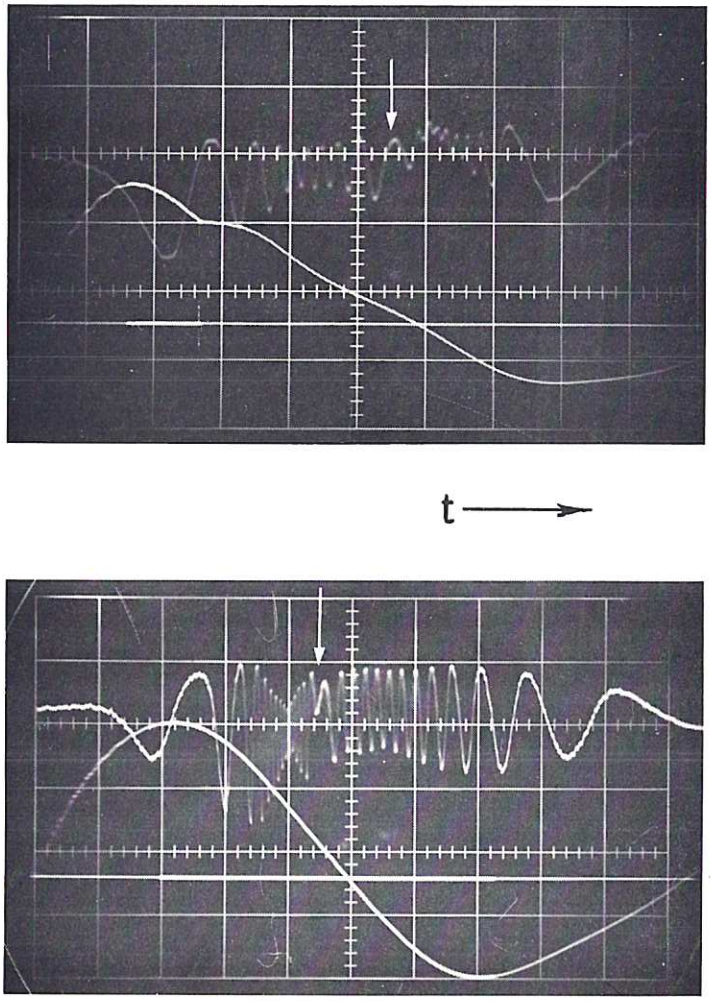

Fig. 4 (CLM-P 208)

For each oscillogram the fringe pattern (top trace) is displayed over a time interval corresponding to the intensified segment on the discharge current waveform (bottom trace). The arrows denote reversal in the direction of change of electron density.

(a) Discharge in 100 torr argon. Fringe pattern 0.2 μsec/div. Discharge current, 2 μsec/div.

(b) Discharge in 1000 torr argon. Fringe pattern 0.2 μsec/div. Discharge current, 2 μsec/div.

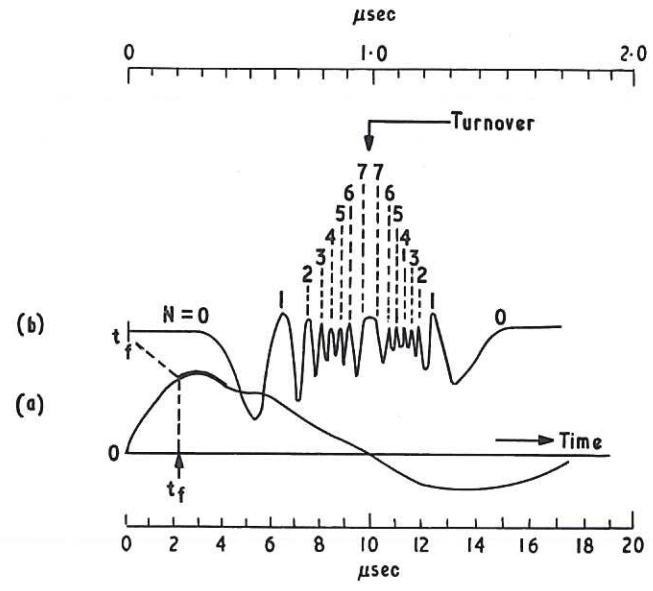

Fig. 5 (CLM-P 208)

Interpretation of the fringe pattern. (a) Discharge current 2 μsec/div. (b) Fringe pattern, 0.2 μsec/div

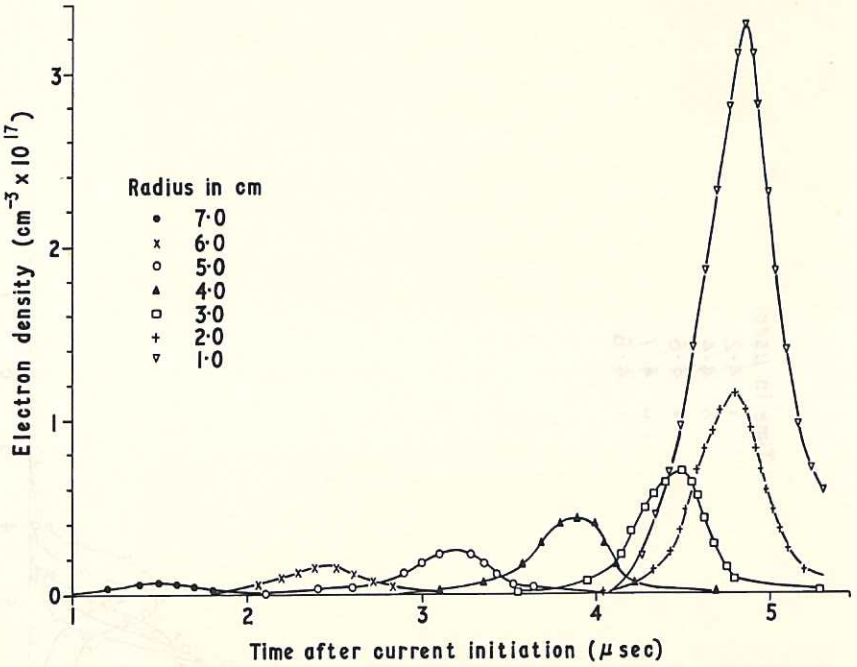

Fig. 6 (CLM-P 208)
Temporal profiles showing electron density (axially integrated) at selected discharge vessel radii for 100 torr argon

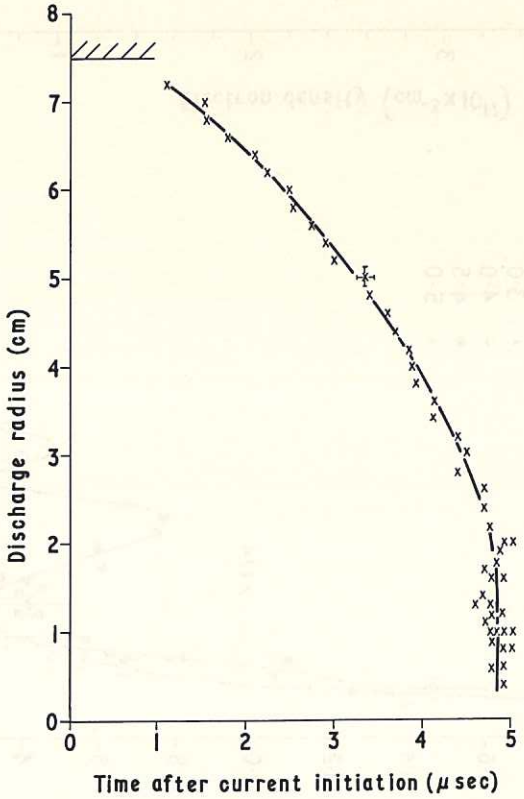

Fig. 7 (CLM-P 208)
Density implosion plot showing radius-vs-time trajectory generated by temporal profile peaks for 100 torr argon

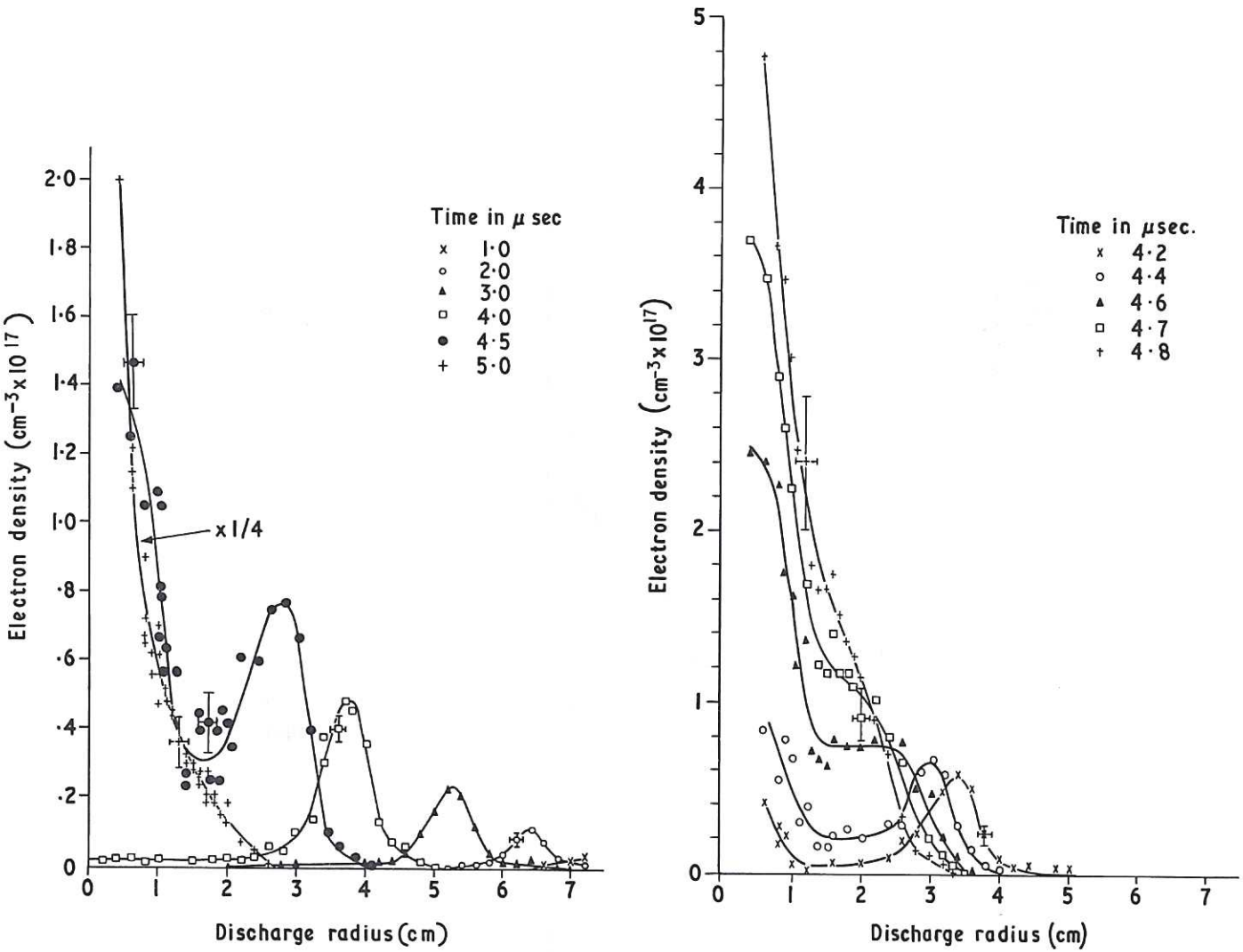

Fig. 8 (CLM-P 208)

Radial profiles showing electron density at selected times after discharge current initiation for 100 torr argon

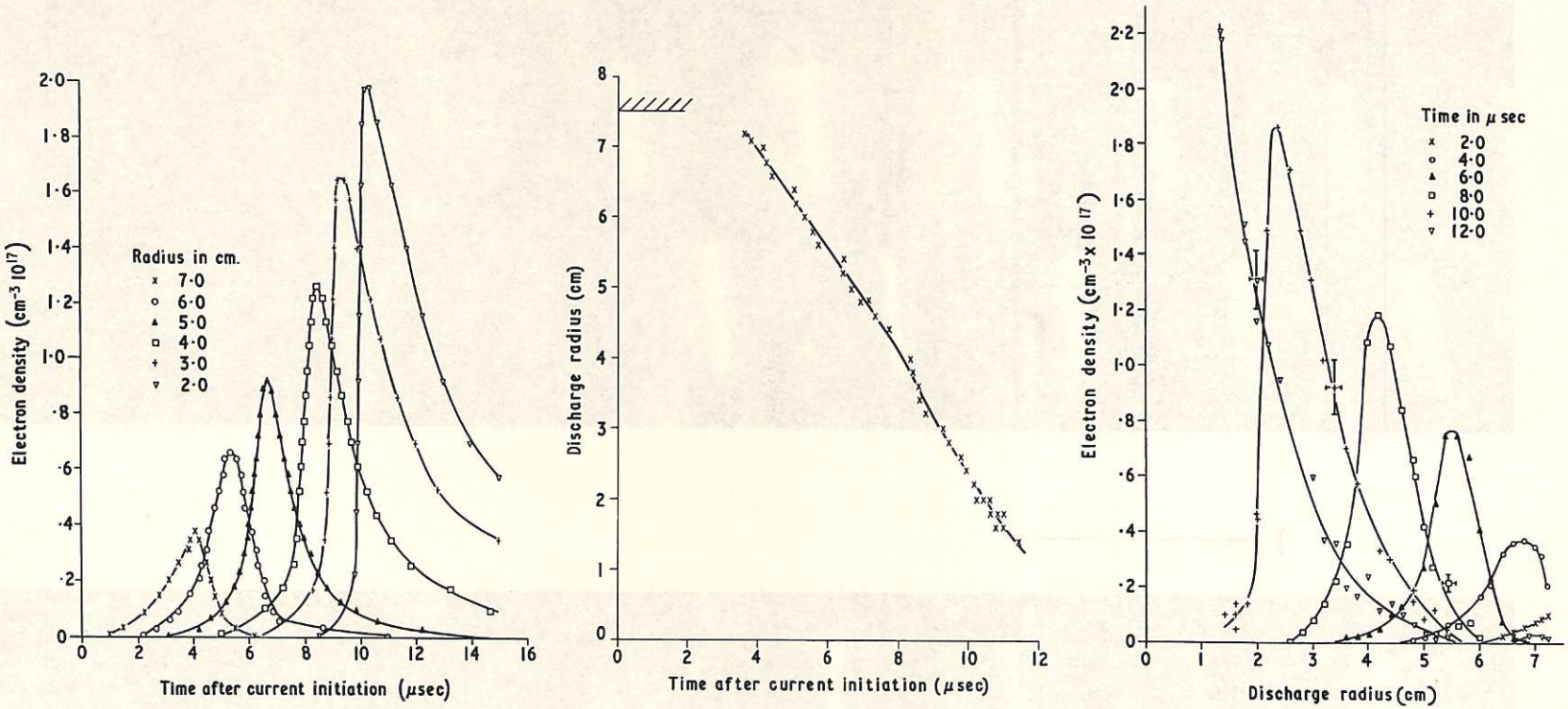

Fig. 9 (CLM-P 208)

Electron density measurements for 1000 torr argon. (a) Temporal profiles; (b) Density implosion curve; (c) Radial profiles

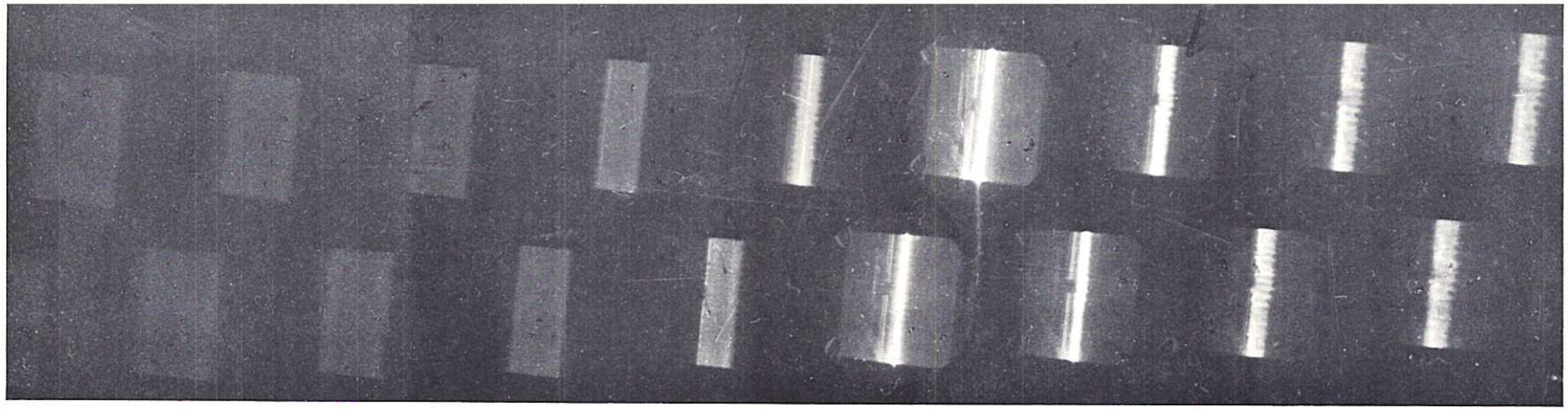

(a)

t

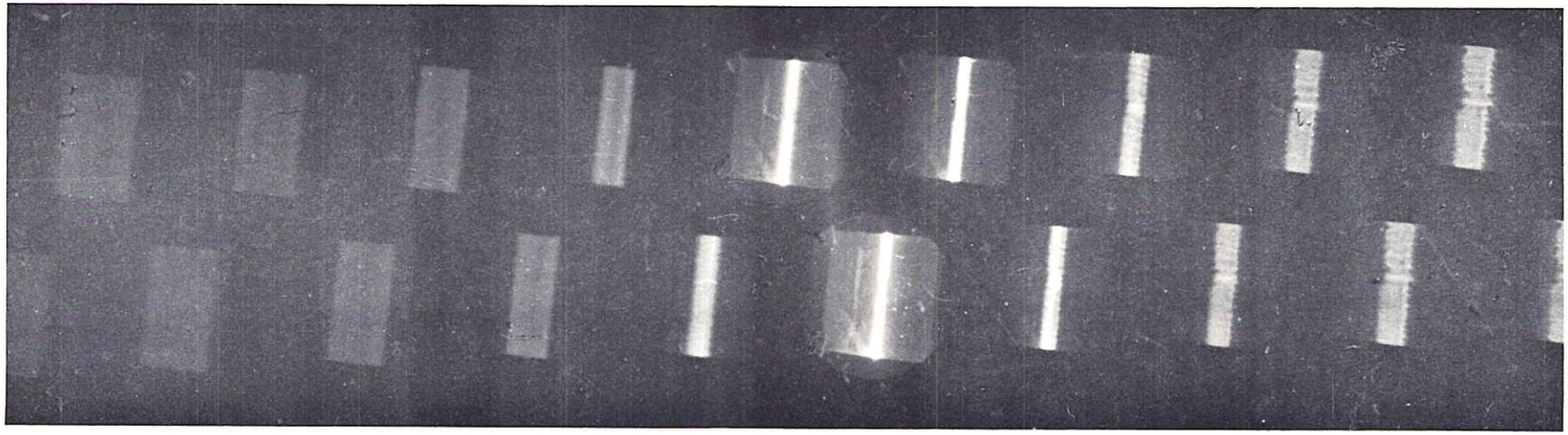

(b)

Fig. 10 (CLM-P 208)

Framing camera photographs showing the z-pinch discharge with the glass tubes inserted to an axial separation of L = 2.5 cm. Successive frames are staggered. Filling pressure, 100 torr argon.

(a) Tubes 2.5 cm from the discharge axis, 0.34 μsec/frame

(b) Tubes nearly coincident with discharge axis, 0.36 μsec/frame